Journal of Alloys and Compounds 509 (2011) 7764–7767

Contents lists available at ScienceDirect

Journal of Alloys and Compounds

journal homepage: www.elsevier.com/locate/jallcom

Magnetocaloric effect of $Fe_{64}Mn_{15-x}Co_xSi_{10}B_{11}$ amorphous alloys

Jong Ho Lee, Seung Jae Lee, Won Bae Han, Hyeun Hwan An, Chong Seung Yoon*

Department of Materials Science and Engineering, Hanyang University, Haengdang-dong, Seongdong-ku, Seoul, 133-791, Republic of Korea

ARTICLE INFO

Article history:
Received 7 March 2011
Received in revised form 26 April 2011
Accepted 27 April 2011
Available online 10 May 2011

Keywords:
Fe–Mn amorphous alloy
Magnetocaloric effect
Magnetic entropy

ABSTRACT

The magnetocaloric effect (MCE) of melt-spun $Fe_{64}Mn_{15-x}Co_xSi_{10}B_{11}$ amorphous alloys with $x = 0$, 0.2, 0.5, 0.7, and 1.0 was evaluated with the aim of maximizing the magnetic entropy change close to the room temperature. The peak magnetic entropy change, $\left|\Delta S_M^{pk}\right|$ for $Fe_{64}Mn_{15}Si_{10}B_{11}$ at 309 K at $H = 15$ kOe was limited to 0.82 J/kg K. The magnetic properties and ensuing MCE were very sensitive to the Co content that it is conjectured that with a smaller amount of Co addition the $\left|\Delta S_M^{pk}\right|$ can be optimized while maintaining the Curie temperature near room temperature. It was also shown that the $Fe_{64}Mn_{15-x}Co_xSi_{10}B_{11}$ amorphous alloys obeyed the master curve behavior as the magnetic entropy change curve collapsed on to a single universal curve.

1. Introduction

The magnetocaloric effect (MCE) which refers to the heating or cooling of a material under external magnetic field was first discovered in 1881 [1]. Since then, the underlying principle of the MCE has been well documented [2–4] and the MCE has been experimentally measured on various material systems. Recent interest in the MCE was sparked by the discovery of giant MCE in $Gd_5Si_2Ge_2$ and related alloys [5–7] and by the potential use of the giant MCE material in the room temperature magnetic refrigeration as the magnetic refrigeration provides advantages over the conventional compression–vaporization technology in terms of energy efficiency and environmental impact. In addition to $Gd_5Si_2Ge_2$, the giant MCE was also observed in $La(Fe_{1-x}Si_x)_{13}$ [8,9], MnAs [10], and $Ni_{2-x}Mn_xGa$ [11]. However, it is difficult to use these materials in practical application of magnetic refrigeration mainly because the high MCE from these materials stems from a first order magnetic phase transition which is liable to produce internal stress due to a large volume change [12] and thermal and magnetic hysteresis [13]. The high material cost and the slow kinetics of the first order phase transition also limits the use of the materials in a magnetic refrigerator. Alternatively, Fe-based magnetic amorphous alloy with low coercivity, high thermal conductivity, and a wide temperature range in which the MCE is observed is a potential candidate material for magnetic refrigeration in spite of their relatively low magnetic entropy change, ΔS_M [14]. The MCE in the amorphous alloys originates from a second order magnetic phase transition near the Curie temperature, T_C. Because the amorphous alloys exist in a metastable state, it is comparatively easy to incorporate multiple transition metal elements to tune the T_C and optimize the MCE at room temperature. In fact, Caballero-Flores et al. have demonstrated that $Fe_{88-2x}Co_xNi_xZr_7B_4Cu_1$ alloys can outperform a Gd-based compound in refrigerant capacity due to the broad ΔS_M curve [15]. A large MCE was also reported from Finemet amorphous alloys [16]. In this work, the MCE from Fe–Mn–Co amorphous alloys, in which Mn was used to lower the T_C to near room temperature, is characterized and the effect of addition of Co in the alloy is evaluated.

2. Experimental details

Buttons of nominal composition $Fe_{64}Mn_{15-x}Co_xSi_{10}B_{11}$ ($x = 0$, 0.2, 0.5, 0.7 and 1) were prepared by arc melting in argon atmosphere. Amorphous $Fe_{64}Mn_{15-x}Co_xSi_{10}B_{11}$ alloy ribbons were fabricated by melt-spinning technique from the button. Typical samples produced were 20 μm thick and 2 mm wide. Composition of the samples was verified with energy-dispersive X-ray spectroscopy. Amorphous nature of the samples was verified using X-ray diffraction. Temperature dependent magnetization curves within a temperature range from 290 to 520 K and room temperature loops were measured using a vibrating sample magnetometer (VSM, Lakeshore).

3. Results and discussion

Fig. 1(a) shows a series of magnetic hysteresis loops obtained at room temperature for the $Fe_{64}Mn_{15-x}Co_xSi_{10}B_{11}$ alloys with $x = 0$, 0.2, 0.5, 0.7 and 1.0. All of the prepared samples were ferromagnetic with near-zero coercivity. The saturation magnetization, M_S of the alloys increased nearly proportional to the Co content. The temperature dependent magnetization (M–T curves) is shown in Fig. 1(b) to illustrate that the T_C also scaled with the Co content. The T_C was estimated from the derivative of the M–T curves is plotted in Fig. 1(c) as a function of the composition together with the

* Corresponding author. Tel.: +82 2 2220 0384; fax: +82 2 2290 1838.
E-mail address: csyoon@hanyang.ac.kr (C.S. Yoon).

0925-8388/$ – see front matter © 2011 Elsevier B.V. All rights reserved.
doi:10.1016/j.jallcom.2011.04.146

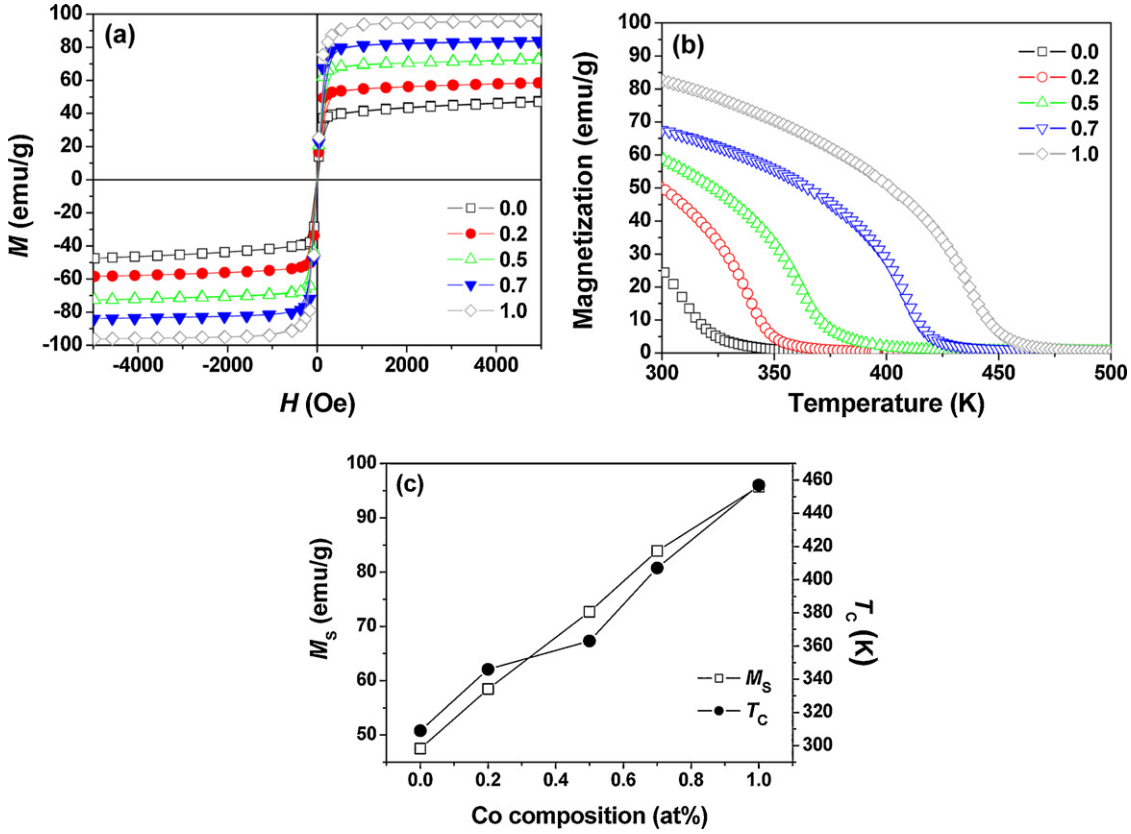

Fig. 1. (a) Magnetic hysteresis loops for the $Fe_{64}Co_xMn_{15-x}Si_{10}B_{11}$ alloys at room temperature, (b) temperature dependent magnetization curves, (c) M_S and T_C plotted against the Co content.

M_S. The T_C and the M_S for $x = 0.0$ agrees well with the $Fe_{80-x}Mn_xB_{20}$ series alloy [17]. Both T_C and M_S increased more or less linearly with the Co content as can be seen from Fig. 1(c). On the average, each 0.1 at.% Co substituting for Mn raised the T_C by 14.8 K and the M_S by 4.8 emu/g. As exchange integrals for both j_{Fe-Mn} and j_{Mn-Mn} are antiferromagnetic [17], replacing of a relatively small amount of Mn with ferromagnetic Co would have a large effect on the magnetic properties of the $Fe_{64}Mn_{15-x}Co_xSi_{10}B_{11}$ alloys. However, the magnitude of the increase is very large compared to other Fe-based amorphous alloys. For example, in the case of $Fe_{80-x}Mn_xB_{20}$ alloys, to raise the T_C by 10 K, approximately 1 at.% of Mn was replaced by Fe [17]. Similarly, in $Fe_{88-2x}Co_xNi_xZr_7B_4Cu1$ alloys, ~30 K rise in the T_C was observed for every 1 at.% addition of Co and Ni [15]. It appears that unlike other amorphous alloys, the magnetic properties of the $Fe_{64}Mn_{15-x}Co_xSi_{10}B_{11}$ alloys were extremely sensitive to the composition, especially to the Co content.

The M–T curves with an applied field of $H = 0.25$–8 kOe were measured for each sample. From the M–T curves, the isothermal magnetic entropy change was numerically estimated using the Maxwell relation [4] and the calculated magnetic entropy with $\Delta H = 8$ kOe is plotted as a function of temperature in Fig. 2(a). The ΔS_M for each sample peaked around its respective T_C and the $\left|\Delta S_M^{pk}\right|$ rose abruptly after the addition of Co and then gradually decreased with increasing Co content. The $\left|\Delta S_M^{pk}\right|$ and the temperature, T_{pk} at which ΔS_M reaches the maximum are tabulated in Table 1 along with other relevant magnetic data. The decrease in $\left|\Delta S_M^{pk}\right|$ for $Fe_{64}Mn_{15-x}Co_xSi_{10}B_{11}$ does not agree with the trend that typically observed in other soft magnetic amorphous alloys. In most soft magnetic amorphous alloys, the increase in the T_{pk} in a series of similar compositions is accompanied by concurrent increase in the $\left|\Delta S_M^{pk}\right|$ [18]. Some of exceptions to the trend were found in $Fe_{91-x}Mo_8Cu_1B_x$ [18], $Fe_{80-x}Cr_8B_{12}Gd_x$ [19], $Fe_{85-x}Zr_{10}B_5Co_x$ [20] for which the $\left|\Delta S_M^{pk}\right|$ either remained constant or decreased as the T_{pk} rose. In those alloys, the reduction in the $\left|\Delta S_M^{pk}\right|$ was attributed to the decrease in the average magnetic moment per atom as Fe was substituted by Gd, B, or Co in those alloys. Meanwhile, the alloying of by Gd, B, or Co pushed their respective T_{pk} (or T_C) to a higher temperature. In our case of $Fe_{64}Mn_{15-x}Co_xSi_{10}B_{11}$, the initial increase in $\left|\Delta S_M^{pk}\right|$ at $x = 0.2$ can be explained by Mn atoms being replaced by ferromagnetic Co atoms which would raise the spontaneous magnetization of the alloy. However, it is not clear why $\left|\Delta S_M^{pk}\right|$ should progressively decrease with further addition of Co which replaced Mn while the Fe fraction was kept constant. It is speculated that the additional Co atoms may have resulted in predominantly Fe–Co bonding which would have lowered the magnetic moment of Fe as observed in $Fe_{80-x}Co_xB_{20}$ amorphous alloys in which relative increase of Co fraction progressively lowered the average magnetic moment [21].

On the other hand, the entropy curve substantially broadened with the increasing Co content. The refrigeration capacity (RC) which approximately quantifies the total heat transferred between the hot and cold reservoirs over the active temperature range [22] was calculated from the product of $\left|\Delta S_M^{pk}\right|$ with the full width at half maximum (FWHM) of the entropy curve for $x = 0.2$, 0.5, 0.7 and 1.0. The calculated RC values are plotted in Fig. 2(b) and tabulated in Table 1. Unlike the $\left|\Delta S_M^{pk}\right|$, the RC increased to a peak value at $x = 1.0$ as the ΔS_M curve for $x = 1.0$ broadened considerably. It is

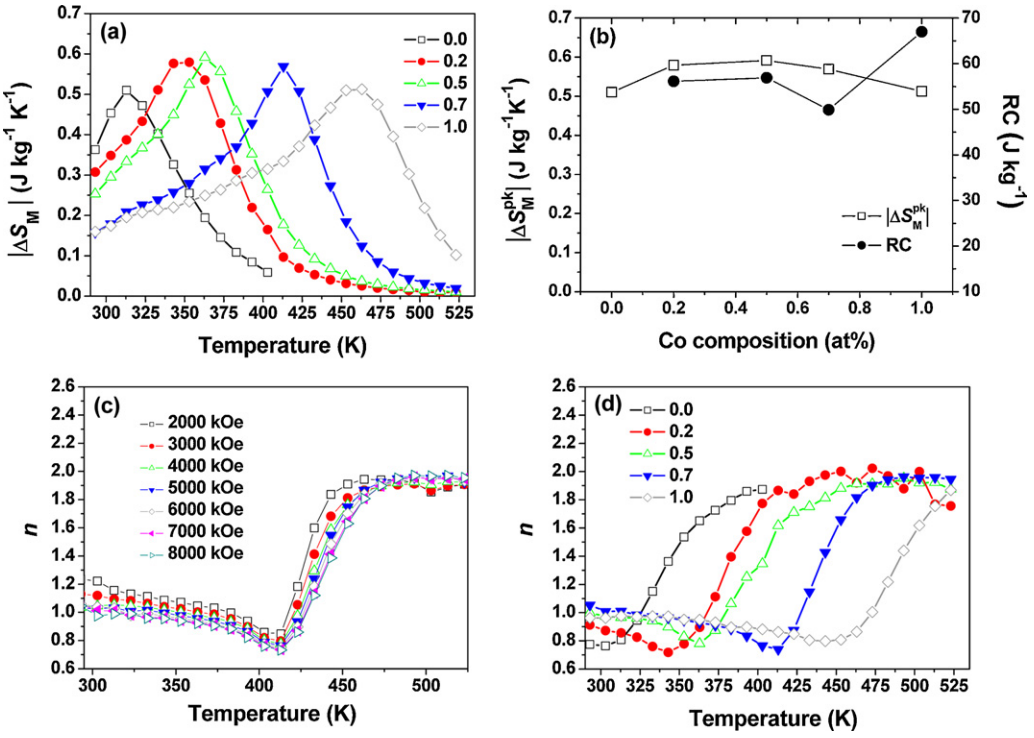

Fig. 2. (a) Temperature dependence of ΔS_M measured with $\Delta H = 8$ kOe for the $Fe_{64}Co_xMn_{15-x}Si_{10}B_{11}$ alloys, (b) $\left|\Delta S_M^{pk}\right|$ and RC as a function of the Co content (c) field exponent, n for $x = 0.7$ as a function of temperature at different external fields, (d) field exponent, n for $Fe_{64}Co_xMn_{15-x}Si_{10}B_{11}$ at 8 kOe.

Table 1
Magnetic and MCE properties for the $Fe_{64}Mn_{15-x}Co_xSi_{10}B_{11}$ alloys.

Composition	M_S (emu/g)	T_C (K)	T_{pk} (K)	$\left\|\Delta S_M^{pk}\right\|$ (J/kg K) ($\Delta H = 8$ kOe)	RC (J/kg) ($\Delta H = 8$ kOe)	n at T_C	$\left\|\Delta S_M^{pk}\right\|$ (J/kg K)($\Delta H = 15$ kOe)
$x = 0.0$	48	309	313	0.51	–	0.76	0.82
$x = 0.2$	59	346	353	0.58	56	0.72	0.92
$x = 0.5$	73	363	363	0.59	57	0.78	0.96
$x = 0.7$	84	409	413	0.57	50	0.74	0.91
$x = 1.0$	96	457	463	0.51	67	0.80	0.83

noted that the MCE of the $Fe_{64}Mn_{15-x}Co_xSi_{10}B_{11}$ alloy was also sensitive to the Co addition as the observed changes in $\left|\Delta S_M^{pk}\right|$ and RC occurred with less than 1 at.% of Co whereas in other alloys, several atomic percentages in composition change were needed to produce noticeable changes in the MCE.

In order to compare the $\left|\Delta S_M^{pk}\right|$ for the present series of alloys with the reported literature values which are typically measured with $H > 10$ kOe, the relationship between the applied field and the $\left|\Delta S_M^{pk}\right|$ was written as $\Delta S_M^{pk}(H) = cH^n$ where c is a constant and n is the field exponent which is independent of the applied field at $T = T_C$ [15]. To estimate n at the T_C, the temperature dependence of the field exponent was calculated from $\frac{d \ln|\Delta S_M|}{d \ln H}$. A typical field exponent, n for $x = 0.7$ as a function of temperature at varying external field is shown in Fig. 2(c). Above the T_C, n was ~2 matching the value calculated from integration of the Curie–Weiss law and decreased to ~1 in the ferromagnetic regime [23]. Near the T_C, n reached the minimum and converged to a single value as expected. The field exponent curves for $x = 0.0$, 0.2, 0.5, 0.7 and 1.0 with an applied field of 8 kOe are plotted in Fig. 2(d). The minimum of the field exponent was around 0.76 as listed in Table 1. The values of n at the T_C for $Fe_{64}Mn_{15-x}Co_xSi_{10}B_{11}$ were substantially larger than $n = 2/3$ predicted from the mean field theory [24], but close to the value reported to other Fe-based soft magnetic alloys [15,18,20].

Using the field exponent estimated from Fig. 2(d), the $\left|\Delta S_M^{pk}\right|$ was extrapolated to $H = 15$ kOe and the $\left|\Delta S_M^{pk}\right|$ ranged from 0.82 to 0.96 J/kg K as can be seen from Table 1. The $\left|\Delta S_M^{pk}\right|$ for $Fe_{64}Mn_{15}Si_{10}B_{11}$ which had its T_{pk} at 309 K at $H = 15$ kOe was 0.82 J/kg K. For comparison, the $\left|\Delta S_M^{pk}\right|$ values near room temperature measured for different magnetic alloys found in the literature are tabulated in Table 2. Although the extrapolated $\left|\Delta S_M^{pk}\right|$ for $Fe_{64}Mn_{15}Si_{10}B_{11}$ belongs in the lower range of the $\left|\Delta S_M^{pk}\right|'s$, the

Table 2
Near room temperature $\left|\Delta S_M^{pk}\right|$ for Fe-based soft magnetic alloys reported in the literature.

Fe-based magnetic alloys	ΔH (kOe)	T_{pk} (K)	$\left\|\Delta S_M^{pk}\right\|$ (J/kg K)
Fe68.5Mo5Si13.5B9Cu1Nb3 [14]	15	469	1.07
Fe88Zr7B4Cu1 [15]	15	295	1.32
Fe65Mn15B20 [17]	15	338	0.89
Fe66Mo8Cu1B15 [18]	15	315	0.92
Fe70Cr8Nb5Cu1Si4B12 [27]	15	284	0.94
Fe63.75Co11.25Nb10B15 [28]	15	440	0.84
Fe86Y5Zr9 [29]	15	285	0.89

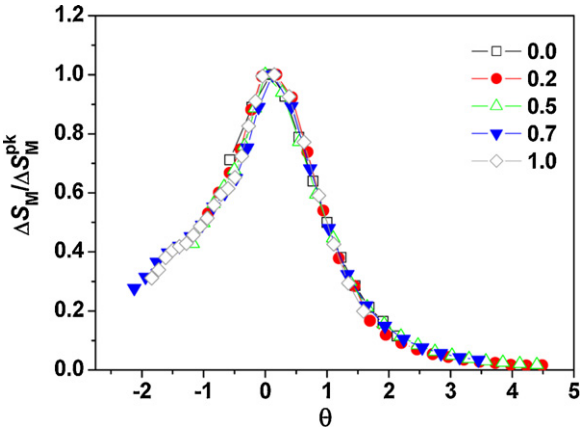

Fig. 3. Rescaled ΔS_M curves of the $Fe_{64}Co_xMn_{15-x}Si_{10}B_{11}$ alloys with $\Delta H = 8$ kOe.

MCE was very sensitive to the composition so that it is conjectured that with a smaller amount of Co addition the $\left|\Delta S_M^{pk}\right|$ can be further optimized while maintaining the T_{pk} near room temperature.

Normalized $\Delta S_M(T)$ curves for alloys in a compositional series have been shown to collapse onto a universal curve for materials with a second order phase transition and the universal curve has been theoretically justified [25,26]. The master curve can be used to estimate the ΔS_M beyond the measured temperature range whose accuracy has been experimentally verified [18]. Fig. 3 shows $\Delta S_M(T)/\Delta S_M^{pk}$ plotted against $\theta = (T-T_C)/(T_r-T_C)$ where T_r is the temperature at which $\Delta S_M(T) = 0.5\Delta S_M^{pk}$. The measured $\Delta S_M(T)$ curves for $Fe_{64}Mn_{15-x}Co_xSi_{10}B_{11}$ indeed collapsed onto a single master curve as can be seen from Fig. 3 as the critical exponents for the alloys were nearly constant regardless of the Co content.

4. Conclusion

The MCE of the $Fe_{64}Mn_{15-x}Co_xSi_{10}B_{11}$ amorphous alloys were evaluated with the aim of maximizing the magnetic entropy change close to the room temperature. It was shown that the MCE response was sensitive to the Co addition so that a small amount of Co addition can be used to tune the Curie temperature and to increase the $\left|\Delta S_M^{pk}\right|$ for possible application of the alloy in magnetic refrigeration.

Acknowledgment

This research was supported by a grant (code #:2010K000356) from 'Center for Nanostructured Materials Technology' under '21st Century Frontier R&D Programs' of the Ministry of Education, Science and Technology, Korea.

References

[1] V.K. Pecharsky, K.A. Gschneidner, J. Magn. Magn. Mater. 200 (1999) 44.
[2] K.H.J. Buschow, Handbook of Magnetic Materials, vol. 12, Elsevier Science B.V., Amsterdam, 1999.
[3] H. Kronmuller, S. Parkin, Handbook of Magnetism and Advanced Magnetic Materials, vol. 4, John Wiley & Sons Ltd., Chichester, 2007.
[4] J.S. Amaral, V.S. Amaral, J. Magn. Magn. Mater. 322 (2010) 1552.
[5] V.K. Pecharsky, A.P. Holm, K.A. Gschneidner, R. Rink, Phys. Rev. Lett. 91 (2003) 197204.
[6] V.K. Pecharsky, G.D. Samolyuk, V.P. Antropov, A.O. Pecharsky, K.A. Gschneidner, J. Solid State Chem. 171 (2003) 57.
[7] A. Yan, A. Handstein, P. Kerschl, K. Nenkov, K.H. Muller, O. Gutfleisch, J. Appl. Phys. 95 (2004) 7064.
[8] S. Fujieda, A. Fujita, K. Fukamichi, Appl. Phys. Lett. 81 (2002) 1276.
[9] A. Fujita, S. Fujieda, Y. Hasegawa, K. Fukamichi, Phys. Rev. B 67 (2003) 1044161.
[10] H. Wada, Y. Tanabe, Appl. Phys. Lett. 79 (2001) 3302.
[11] A.A. Cherechukin, T. Takagi, M. Matsumoto, V.D. Buchel'nikov, Phys. Lett. A 326 (2004) 146.
[12] M. Nazih, A. de Visser, L. Zhang, O. Tegus, E. Bru¨ck, Solid State Commun. 126 (2003) 255.
[13] V. Provenzano, A.J. Shapiro, R.D. Shull, Nature 429 (2004) 853.
[14] V. Franco, J.S. Blazquez, M. Millán, J.M. Borrego, C.F. Conde, A. Conde, J. Appl. Phys. 101 (2007) 09C053.
[15] R. Caballero-Flores, V. Franco, A. Conde, K.E. Knipling, M.A. Willard, Appl. Phys. Lett. 96 (2010) 182506.
[16] N. Chau, N.D. The, N.Q. Hoa, C.X. Huu, N.D. Tho, S.C. Yu, Mater. Sci. Eng. A 449 (2007) 360.
[17] R. Caballero-Flores, V. Franco, A. Conde, L.F. Kiss, J. Appl. Phys. 108 (2010) 073921.
[18] V. Franco, C.F. Conde, J.S. Blázquez, A. Conde, P. Švec, D. Janičkovič, L.F. Kiss, J. Appl. Phys. 101 (2007) 093903.
[19] J.Y. Law, R.V. Ramanujan, V. Franco, J. Alloys Compd. 508 (2010) 14.
[20] Y.K. Fang, C.C. Yeh, C.C. Hsieh, C.W. Chang, H.W. Chang, W.C. Chang, X.M. Li, W. Li, J. Appl. Phys. 105 (2009), 07A910.
[21] E.P. Wohlfarth, Ferromagnetic Materials, vol. 1, North-Holland Publishing Company, Amsterdam, 1980.
[22] V.M. Prida, V. Franco, V. Vegaa, J.L. Sanchez-Llamazares, J.J. Suñol, A. Conde, B. Hernando, J. Alloys Compd. 509 (2011) 190.
[23] T.D. Shen, R.B. Schwarz, J.Y. Coulter, J.D. Thompson, J. Appl. Phys. 91 (2002) 5240.
[24] H. Oesterreicher, F.T. Parker, J. Appl. Phys. 55 (1984) 4334.
[25] V. Franco, J.S. Blazquez, A. Conde, Appl. Phys. Lett. 89 (2006) 222512.
[26] V. Franco, A. Conde, Int. J. Refrig. 33 (2010) 465.
[27] A. Kolano-Buriana, M. Kowalczykb, R. Kolanoa, R. Szymczakc, H. Szymczakc, M. polak, J. Alloys Compd. 479 (2009) 71.
[28] J.J. Ipus, J.S. Blazquez, V. Franco, A. Conde, J. Alloys Compd. 496 (2010) 7.
[29] K.S. Kim, S.G. Min, S.C. Yu, S.K. Oh, Y.C. Kim, K.Y. Kim, J. Magn. Magn. Mater. 304 (2006), e642.